

# Bioinformatics analysis and experimental verification of NLRX1 as a prognostic factor for esophageal squamous cell carcinoma

LU ZHOU\*, LANLAN GAN\*, CHEN SUN, ALAN CHU, MENGLIN YANG and ZONGWEN LIU

Tumor Radiotherapy Department, The Second Affiliated Hospital, Zhengzhou University, Zhengzhou, Henan 450000, P.R. China

Received November 22, 2023; Accepted March 26, 2024

DOI: 10.3892/ol.2024.14397

**Abstract.** Nucleotide binding and oligomeric domain-like receptor X1 (NLRX1), a member of the NLR family, is associated with the physiological and pathological processes of inflammation, autophagy, immunity, metabolism and mitochondrial regulation, and has been demonstrated to have pro- or antitumor effects in various tumor types. However, the biological function of NLRX1 in esophageal squamous cell carcinoma (ESCC) has remained elusive. In the present study, by using bioinformatics methods, the differential expression of NLRX1 at the mRNA level was examined. Overall survival, clinical correlation, receiver operating characteristic curve, Cox regression, co-expression, enrichment, immune infiltration and drug sensitivity analyses were carried out. A nomogram and a calibration curve were constructed. Changes in protein expression levels were investigated by immunohistochemistry and western blotting. The impact of NLRX1 on i) cell proliferation was evaluated by Cell Counting Kit-8 assays; ii) migration was examined by wound-healing assays; iii) migration and invasion were evaluated by Transwell assays; and iv) apoptosis was assessed by Annexin V/PI staining and flow cytometry. The results revealed that, compared to normal adjacent tissue, NLRX1 was lowly expressed in ESCC, and patients with low NLRX1 expression had a shorter survival time. NLRX1 was an independent prognostic factor for ESCC and was associated

with tumor grading. Patients in the low-NLRX1 group showed a decrease in the infiltration of activated natural killer cells, monocytes and M0 macrophages, and these immune-cell infiltration levels were positively correlated with NLRX1 expression. Knocking down NLRX1 promoted the proliferation of KYSE450 cells, while overexpression of NLRX1 inhibited the proliferation of ECA109 cells. NLRX1 negatively regulated the PI3K/AKT signaling pathway in ESCC. These findings indicate that, through several mechanisms, NLRX1 suppresses tumor growth in ESCC, which offers new insight for investigating the causes and progression of ESCC, as well as for identifying more efficient therapeutic approaches.

## Introduction

Esophageal cancer (EC) is the 10th most prevalent malignancy worldwide and the seventh leading cause of cancer-associated mortalities. According to statistics, in 2020, there were 604,100 new cases of and 544,076 deaths from esophageal cancer worldwide (1). The most prevalent histological form of EC, squamous cell carcinoma (SCC), accounts for ~85% of all cases globally (2). Despite the advances in medical technology, the prognosis for patients with esophageal SCC (ESCC) remains unsatisfactory (3). Understanding the molecules involved in the development of ESCC may lead to new insight for developing methods of improving patient prognosis.

During the last 20 years, 22 human and 34 mouse members of the nucleotide binding and oligomeric domain-like receptor (NLR) family have been identified (4). The sole NLR member found in mitochondria is NLRX1, a member of the NLRC subfamily. It is involved in immune, inflammatory, autophagic, mitochondrial regulatory and metabolic processes (5). In addition, NLRX1 is associated with the initiation and progression of cancer (6-9). In an azomethane (AOM)-induced colorectal cancer model, as well as in estrogen receptor (ER)/progesterone receptor (PR)- breast cancer and in human papilloma-virus-induced head and neck SCC, it has been reported that NLRX1 can enhance tumor growth. NLRX1 can also slow down the growth of pancreatic cancer, ER/PR+ breast cancer, hepatocellular carcinoma, histiocyte sarcoma and a dextran sodium sulfate/AOM-induced colitis model (6,7,10-14). This suggests that NLRX1 can stimulate or repress tumor growth via as-yet-unidentified mechanisms. However, the association between NLRX1 and ESCC has so far remained elusive.

*Correspondence to:* Professor Zongwen Liu, Tumor Radiotherapy Department, The Second Affiliated Hospital, Zhengzhou University, 8 Jingba Road, Zhengzhou, Henan 450000, P.R. China  
E-mail: liuzwhh@sina.com

\*Contributed equally

**Abbreviations:** NLRX1, nucleotide binding and oligomeric domain-like receptor X1; ESCC, esophageal squamous cell carcinoma; OS, overall survival; ROC, receiver operating characteristic; WB, western blot; AOM, azomethane; GEO, Gene Expression Omnibus; TCGA, The Cancer Genome Atlas; GSEA, Gene Set Variation Analysis; OD, optical density; GO, Gene Ontology; GSEA, Gene Set Enrichment Analysis; KEGG, Kyoto Encyclopedia of Genes and Genomes

**Key words:** ESCC, NLRX1, immune infiltration, bioinformatics

The present study aimed to identify potential links between NLRX1 and ESCC. First, bioinformatics were used to examine NLRX1 expression, prognosis, potential biological activities, interaction with immune infiltration and treatment sensitivity in ESCC. Next, *in vitro* assays were performed to investigate the possible biological function of NLRX1 in ESCC. The present findings imply that NLRX1 may be a crucial tumor suppressor in ESCC.

## Materials and methods

**Data and patient specimen collection.** From the Gene Expression Omnibus (GEO) database (<https://www.ncbi.nlm.nih.gov/geo/>), the ESCC gene expression datasets GSE20347, GSE23400, GSE53625, GSE67269 and GSE161533 were downloaded (15-18). Furthermore, information on the gene expression and survival of 95 patients with ESCC was gathered from The Cancer Genome Atlas (TCGA; <https://cancergenome.nih.gov/>). R v4.2.1 software was used for analysis in the current study (19,20). All transcriptome data underwent the necessary preprocessing before statistical analysis, including averaging multiple expression values of the same gene in each dataset, followed by logarithmic transformation and normalization of the dataset using the R package ‘limma’ (21).

Furthermore, paraffin blocks of cancerous and healthy tissues adjacent to the tumor were collected from patients with ESCC who visited The Second Affiliated Hospital of Zhengzhou University (Zhengzhou, China) between January 2022 and March 2023. The inclusion criteria were as follows: All patients had ESCC, were aged 18-75 years, all surgical specimens had been taken before any neo-adjuvant anti-tumor treatment and all patients had corresponding informed consent. Exclusion criteria were the presence of other malignant tumors, psychological abnormalities or contraindications to anti-tumor treatment.

**Cell lines and culture.** ECA109 and KYSE450 cells were obtained from the American Type Culture Collection, while KYSE150 cells were purchased from Shanghai Zhongqiao Xinzhou Biotechnology Co., Ltd. The culture medium used contained 89% RPMI 1640 medium (cat. no. ZQ0449; Zhongqiao Xinzhou Biotechnology Co., Ltd.), 10% fetal bovine serum (cat. no. 04-001-1ACS; Biological Industries), 1% 100 IU/ml penicillin and 100 g/ml streptomycin (cat. no. CSP006; Zhongqiao Xinzhou Biotechnology Co., Ltd.). Cells were cultured at 37°C and 5% CO<sub>2</sub> saturated humidity.

**Expression and clinical correlation analysis of NLRX1.** First, the ‘limma’ package was used to perform differential analysis on the transcriptome data of the datasets. Next, patients with ESCC in the GSE53625 and the TCGA dataset containing clinical data were divided into two groups using the median expression value of NLRX1: GSE53625 high: n=89, low: n=90; and TCGA high: n=47, low: n=48. Subsequently, Kaplan-Meier survival analysis was performed on them.

The GSE53625 dataset, which had the largest sample size, was used for subsequent analysis using the Wilcoxon signed-rank or  $\chi^2$  tests to analyze the relationship between NLRX1 and clinical reference data. Subsequently, a receiver

operating characteristic (ROC) curve was plotted to evaluate the diagnostic value of NLRX1, and Cox regression analysis was used to help judge the prognostic value of NLRX1. Finally, the ‘survival’ package was used for regression analysis. A nomogram was constructed and a calibration curve was drawn to verify its reliability.

**Enrichment and variation analysis.** First, based on the transcriptome data of the GSE53625 dataset, the correlation between NLRX1 and the expression of other genes was analyzed, and genes highly correlated with NLRX1 were identified with  $|correlation\ coefficient| > 0.5$  and  $P < 0.05$  as selection criteria. Next, Gene Ontology (GO) and Kyoto Encyclopedia of Genes and Genomes (KEGG)-enrichment analyses were performed on these genes, while Gene Set Enrichment Analysis (GSEA) and Gene Set Variation Analysis (GSVA) were used to explore the pathways enriched in the low expression group of NLRX1 in GSE53625. This step utilized the ‘clusterProfiler’, ‘GSEABase’ and ‘GSVA’ packages.

**Immune and drug correlation analysis.** Based on the data from GSE53625, patients were divided into high and low groups according to the median expression value of the NLRX1, and immune-related functional analysis was performed using the ‘GSEABase’ and ‘GSVA’ packages (22,23). Next, the ‘Corrplot’ package was used for immune checkpoint correlation analysis, while the ‘CIBERSORT’ package was used to analyze the degree of immune infiltration in samples and screen out meaningful samples for differential analysis and correlation testing. Finally, from the Genomics of Drug Sensitivity in Cancer website (<https://www.cancerrxgene.org/>), drug information was downloaded and differences in drug sensitivity between patients with high and low expression of NLRX1 were analyzed.

**Immunohistochemical staining.** Immunohistochemical staining was performed as previously described (24). In brief, paraffin-embedded tissues were dewaxed, hydrated and subjected to antigen retrieval and blocking of endogenous peroxidase prior to incubation with anti-NLRX1 antibody (1:200 dilution; cat. no. ab107611; Abcam) at room temperature for 30 min. Next, a conjugated secondary antibody was added (1:100 dilution; cat. no. SA00001-2; Proteintech Group, Inc.) and incubated at room temperature for 30 min, followed by staining with DAB, hematoxylin and alkaline bluing solution. Next, a neutral resin was applied for sealing after dehydration before observing the slides under an optical microscope at x200 magnification and acquiring images.

A semi-quantitative scoring technique based on the percentage of positive cells and staining intensity was used to grade the immunohistochemical staining results as follows: 0, negative staining; 1, pale yellow (weak); 2, yellow (moderate); and 3, brown (strong). The positivity score was assigned as 0 for <5% positive cells; 1 for 6-25% positive cells; 2 for 26-50% positive cells; 3 for 51-75% positive cells; and 4 for >75% positive cells. The two aforementioned scores were then multiplied and 0 was considered to indicate negative expression, <5 low expression and  $\geq 5$  high expression. Two pathologists independently evaluated the immunohistochemical staining.

**Cell transfection and plasmid extraction.** The plasmids (pcDNA3.1-NLRX1) and small interfering RNAs (siRNAs) used in the present study were produced by TsingKe Biological Technology and plasmid extraction was carried out in line with the instructions provided by the manufacturer of FastPure EndoFree Plasmid Mini Kit (cat. no. DC203-01; Vazyme Biotech Co., Ltd.). Approximately  $4 \times 10^5$  KYSE450 cells or  $3 \times 10^5$  EAC109 cells were seeded into 6-well plates and transfection was performed the following day when the cell density reached 70–80%. Transfection was carried out according to the manufacturer's instructions of Lipo8000 transfection reagent (cat. no. C0533; Beyotime Institute of Biotechnology) and subsequent experiments were conducted within 48 h. The siRNA sequences were as follows: siNLRX1 forward, 5'-GGACUACUACAACGAUGAUTT-3' and reverse, 5'-AUCAUCGUUGUAGUAGUCCTT-3'; and negative control (NC) forward, 5'-UUCUCCGAACGUGUCACGUTT-3' and reverse, 5'-ACGUGACACGUUCGGAGAATT-3'.

**Western blot (WB) analysis.** RIPA lysis buffer (cat. no. R0010; Solarbio Group, Inc.) was used to lyse cells, and protein was quantified using the BCA method. Total protein (20  $\mu$ g of protein was added to each lane) was separated by 7.5% SDS-PAGE prepared according to the instructions of the Epizyme PAGE Gel Express Preparation Kit (cat. no. PG111; Epizyme, Inc.; Ipsen Biopharmaceuticals, Inc.). The electrophoresis and PVDF membrane transfer times were adjusted according to the molecular weight of the proteins. A fastblocking solution (cat. no. G2052; Wuhan Servicebio Technology Co., Ltd.) was used to block the membrane at room temperature for 10 min, while an antibody diluent (cat. no. BMU103-CN; Abbkine Scientific Co., Ltd.) was used to dilute the primary antibodies to an appropriate concentration prior to incubation at 4°C overnight. Next, the membrane was incubated with a secondary antibody at room temperature for 2 h. The expression of proteins was then visualized by enhanced chemiluminescence agents (cat. no. BMU102-CN; Abbkine Scientific Co., Ltd.). Anti-NLRX1 (1:1,000 dilution; cat. no. ab107611; Abcam), anti-PI3K/AKT signaling pathway panel (1:1,000; cat. no. ab283852; Abcam) and anti-GAPDH (1:10,000; cat. no. 10494-1-AP; Proteintech Group, Inc.) were used as primary antibodies. The phosphorylation sites of phosphorylated (p)-AKT were S472, S473 and S474, and anti-GAPDH was used as a loading control for normalization. HRP-conjugated Affinipure goat anti-rabbit IgG (H+L) (1:2,000; cat. no. SA00001-2; Proteintech Group, Inc.) was used as the secondary antibody.

**Cell proliferation assay.** For the cell-proliferation experiment, cells transfected on a 6-well culture plate were collected and 2,000 cells per well were added to a fresh 96-well culture plate. When the cells had adhered to the wall after 6 h of incubation, 10  $\mu$ l Cell Counting Kit-8 (CCK-8) reagent (cat. no. BMU106-CN; Abbkine Scientific Co., Ltd.) was added. After 2 h, the optical density (OD) values at 450 nm were measured by a microplate reader (Thermo Fisher Scientific, Inc.) and considered as time=0 h. Next, the OD values at 450 nm were measured at 24, 48 and 72 h.

**Wound-healing assay.** At the back of a 6-well culture plate, three horizontal lines were drawn in advance with a black pen,

while three vertical lines were drawn on the 6-well culture plate with a pipette tip at 48 h post-transfection (cell confluence rate reached >90%) (25). Cells were cultured in medium containing 2% serum (26) and the migration of cells at the intersection of the horizontal and vertical lines was recorded at 0, 24, 48 and 72 h. Results were calculated as Mobility (%)=(A0-AN)/A0, where A0 represents the initial wound width and AN represents the remaining wound width at the metering point.

**Transwell assays.** In the Transwell migration assay, cells were collected and resuspended in serum-free medium and 40,000 cells/200  $\mu$ l were added to each upper chamber of a Transwell plate (8.0- $\mu$ m pore size; Corning, Inc.), while 600  $\mu$ l complete medium was added to each lower chamber. After 36 h, the cells were fixed at room temperature for 30 min with 4% paraformaldehyde and then stained at room temperature for 10 min with crystal violet. After staining, the cells at the top of the pore filter were gently wiped off with a wet cotton swab. The number of migrated cells was observed under a microscope. For the invasion assay, the culture medium was replaced with serum-free culture medium for starvation treatment 1 day in advance. Next, Matrigel® (cat. no. 356234; BD Biosciences) was diluted with serum-free medium and 100  $\mu$ l of this solution was added to each well. After incubation at 37°C for 1 h, any uncured diluent was aspirated and the next steps were the same as for the migration assay.

**Apoptosis analysis.** Approximately  $1 \times 10^5$  KYSE450 cells or  $7.5 \times 10^4$  ECA109 cells into were inoculated in each well of a 24-well plate. According to the instructions of the manufacturer of the apoptosis kit (cat. no. KTA0002; Abbkine Scientific Co., Ltd.), a mixture was prepared at a ratio of apoptosis inducer to complete culture medium of 1:3,000. After 48 h of transfection, 1 ml mixture was added to KYSE450 or ECA109 cells cultured in a 24-well culture plate. After 24 h of induction, Annexin V/PI staining reagent was added and the fluorescence emission of the sample on the slide was observed using a fluorescence microscope. Green fluorescence (Annexin V) represents cell membrane staining and red fluorescence [propidium iodide (PI)] represents cell nuclear staining. Cells exhibiting only green fluorescence represented early apoptotic cells, while cells exhibiting only red fluorescence represented necrotic cells and cells exhibiting both red and green fluorescence represented late apoptotic cells. Furthermore, the cells treated with the above-mentioned kit were prepared into a suspension and analyzed by flow cytometry (BeamCyte Flow Cytometer; Bidake Biotechnology Co., Ltd.), with 10,000 effective cells recorded each time to detect the apoptosis rate, and the software used was CytoSYS v1.0 (Bidake Biotechnology Co., Ltd.).

**Statistical analysis.** SPSS 26.0 (IBM Corp.) was used for statistical analysis. Each experiment was performed as 3 repeats. Continuous variables were presented as the mean  $\pm$  standard error of the mean. To determine the significance of the difference between the two groups, an unpaired Student's t-test, Fisher's exact test or  $\chi^2$  test was employed as appropriate. If the variances within the groups were not homogenous, nonparametric Mann-Whitney U or Wilcoxon signed-rank tests



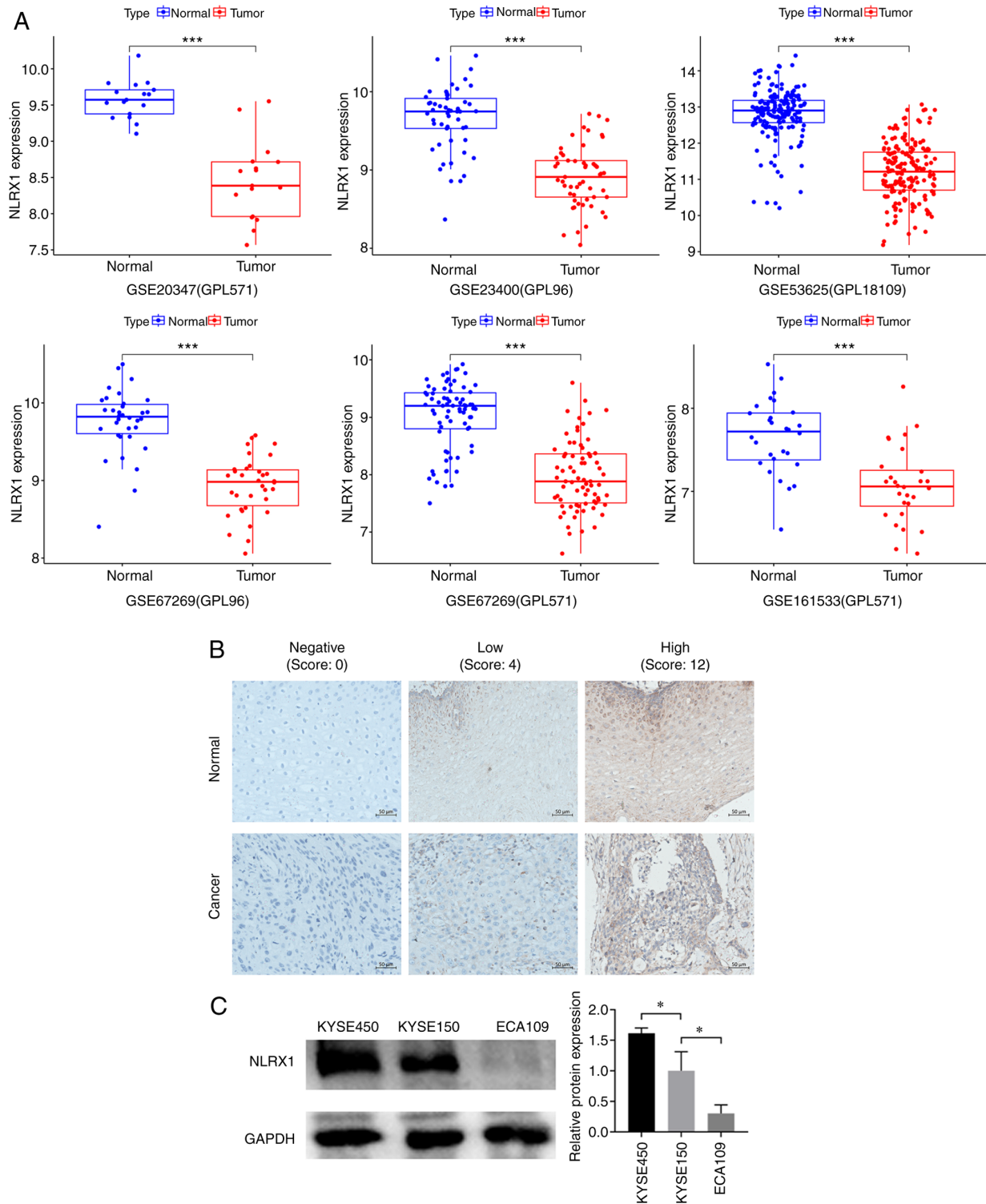


Figure 1. Expression of NLRX1 at mRNA and protein levels. (A) Differences in mRNA expression of NLRX1 in six datasets. (B) Typical immunohistochemistry images (scale bars, 50 μm). (C) Protein-level expression of NLRX1 in esophageal squamous cell carcinoma cell lines KYSE450, KYSE150, and ECA109. \*P<0.05, \*\*\*P<0.001. NLRX1, nucleotide binding and oligomeric domain-like receptor X1.

were used. P<0.05 was considered to indicate a statistically significant difference.

## Results

*Expression of NLRX1 at the mRNA and protein levels.* Data mining revealed that, in contrast to normal adjacent tissue,

NLRX1 was expressed at lower mRNA levels in ESCC tissue (Fig. 1A). To determine whether there were changes in the expression of NLRX1 at the protein level in 36 pairs of cancerous and adjacent normal tissues [24 males and 12 females; 11 patients aged <65 years and 25 patients aged ≥65 years; median age, 68 years (range, 18-75 years), immunohistochemistry was employed (Fig. 1B). The results showed



that NLRX1 protein expression was lower in cancer tissues (19 cases of low expression) than in adjacent normal tissues (10 cases of low expression), with a statistically significant difference ( $\chi^2=4.677$ ,  $P=0.031$ , Table I).

Among the KYSE450, KYSE150 and ECA109 cell lines, NLRX1 expression was higher in KYSE450 cells, while the expression level of NLRX1 in ECA109 cells was lower ( $P<0.05$  vs. KYSE150; Fig. 1C). Therefore, in subsequent experiments, NLRX1 expression was knocked down in KYSE450 cells and overexpressed in ECA109 cells.

**Clinical and prognostic value of NLRX1 in ESCC.** Patients with low NLRX1 levels had shorter survival times in the GSE53625 and TCGA datasets (Fig. 2A). An association between NLRX1 and the pathological parameter of tumor grade was found in patients with ESCC (Fig. 2B). In the ROC curve, the area under the curve of NLRX1 expression was 0.933, indicating that NLRX1 has a good diagnostic value (Fig. 2C). Univariate and multivariate Cox regression analyses showed that NLRX1 was an independent prognostic factor for OS with a hazard ratio of 0.726 [95% confidence interval (CI), 0.574-0.919] and 0.770 (95% CI, 0.596-0.995), respectively (Fig. 2D). Next, a nomogram was created based on the NLRX1 expression and clinical data contained in the GSE53625 dataset as parameters to predict the prognosis of patients with ESCC. The calibration curves of OS showed good consistency between the predicted OS and the observed OS, indicating that the predicted results of the nomogram are in good agreement with the actual results (Fig. 2E).

**Identification of relevant genes for NLRX1 and enrichment analysis.** Based on co-expression analysis, 181 genes were found to be highly correlated with NLRX1 (Table SI), and Circos plots were used to show the 6 genes that were most positively correlated with NLRX1 and the 5 genes that were most negatively correlated with NLRX1 (Fig. 3A). In the KEGG analysis, NLRX1-related genes were mainly enriched in 'phagosome', 'arachidonic acid metabolism' and 'endocytosis', while in the GO analysis, they were mainly enriched in 'skin development', 'cornified envelope' and 'structural constituent of skin epidermis' (Fig. 3B).

Next, the tumor samples of GSE53625 were divided into two groups according to the median expression value of NLRX1, and GSEA and GSVA were performed. The results showed that pathways/functional terms including 'taste transduction', 'arrhythmogenic right ventricular cardiomyopathy', 'melanoma', 'focal adhesion', 'small cell lung cancer', 'antigen processing and presentation', 'prostate cancer', 'stem cell differentiation', 'polymerase II specific DNA binding transcription factor binding' and 'histone binding' were enriched in the NLRX1 low expression group ( $n=90$ ) ( $P<0.05$ ; Fig. 3C and D).

**Immunological and drug sensitivity analysis.** To investigate whether NLRX1 is immune-related in ESCC, an immune-related functional analysis was first performed. The findings demonstrated that in 179 ESCC samples, the group with low NLRX1 expression ( $n=90$ ) had lower scores for CC chemokine receptors (CCR), dendritic cells (DCs), plasma-like dendritic cells (pDCs) and T-cell co-stimulation (Fig. 4A,  $P<0.05$ ; Table SII contains definitions of the terms).

Table I. Expression of NLRX1 in esophageal squamous cell carcinoma and normal tissues.

Group	Cancer (n=36)	Normal (n=36)	$\chi^2$	P-value
NLRX1			4.677	0.031
Low	19	10		
High	17	26		

NLRX1, nucleotide binding and oligomeric domain-like receptor X1.

Afterward, 85 meaningful samples ( $P<0.05$ ) were analyzed using the 'CIBERSORT' package for immune infiltration analysis. According to the median expression value of NLRX1, they were divided into two groups. In the differential analysis and correlation testing, the degree of natural killer (NK) cells activated, monocytes and macrophages M0 infiltration decreased in the low NLRX1 group ( $n=43$ ) and was highly positively correlated with NLRX1 expression (Fig. 4B and C). Immunological checkpoint analysis showed that TNFRSF25, TNFSF9, TMIGD2, CD244, TNFRSF18, HHLA2, PDCD1, TNFRSF4, CD40LG and CD86 were positively correlated with NLRX1, while ICOSLG, TNFSF15, CD80, CD276, BTLA, CD200R1 and CTLA4 were negatively correlated with NLRX1 (Fig. 4D,  $P<0.05$ ). Drug sensitivity analysis revealed that the group with low NLRX1 expression was more resistant to 5-fluorouracil and more sensitive to irinotecan (Fig. 4E).

**Downregulation of NLRX1 expression promotes the growth and development of KYSE450 cells.** In order to further explore the biological function of NLRX1 in ESCC, *in vitro* experiments were conducted. As confirmed by WB, the expression of NLRX1 was knocked down in KYSE450 cells (Fig. 5A). The results of the CCK8 assay showed that knockdown of NLRX1 significantly promoted the growth of KYSE450 cells (Fig. 5B,  $P<0.05$ ). Furthermore, the scratch wound-healing and Transwell assays showed that silencing NLRX1 expression significantly promoted the migration and invasion of KYSE450 cells (Fig. 5C and D,  $P<0.05$ ). The fluorescence microscopy and flow cytometry results of the apoptosis experiment also showed that knockdown of NLRX1 significantly reduced the apoptosis of KYSE450 cells (Fig. 5E,  $P<0.05$ ).

**Upregulation of NLRX1 expression inhibits the growth and development of ECA109 cells.** In ECA109 cells, NLRX1 was overexpressed (Fig. 6A). According to our findings, upregulation of NLRX1 expression in ECA109 cells significantly inhibited cell growth, migration and invasion, and significantly increased apoptosis (Fig. 6B-E,  $P<0.05$ ).

**NLRX1 regulates the PI3K/AKT signaling pathway in ESCC.** To further explore the mechanism by which NLRX1 regulates the growth and development of ESCC, we experimentally analyzed the effects of NLRX1 on the PI3K/AKT pathway. According to the WB data, silencing NLRX1 in KYSE450 significantly activated the PI3K/AKT pathway (Fig. 7A,  $P<0.05$ ). By contrast, upregulation of NLRX1 in ECA109

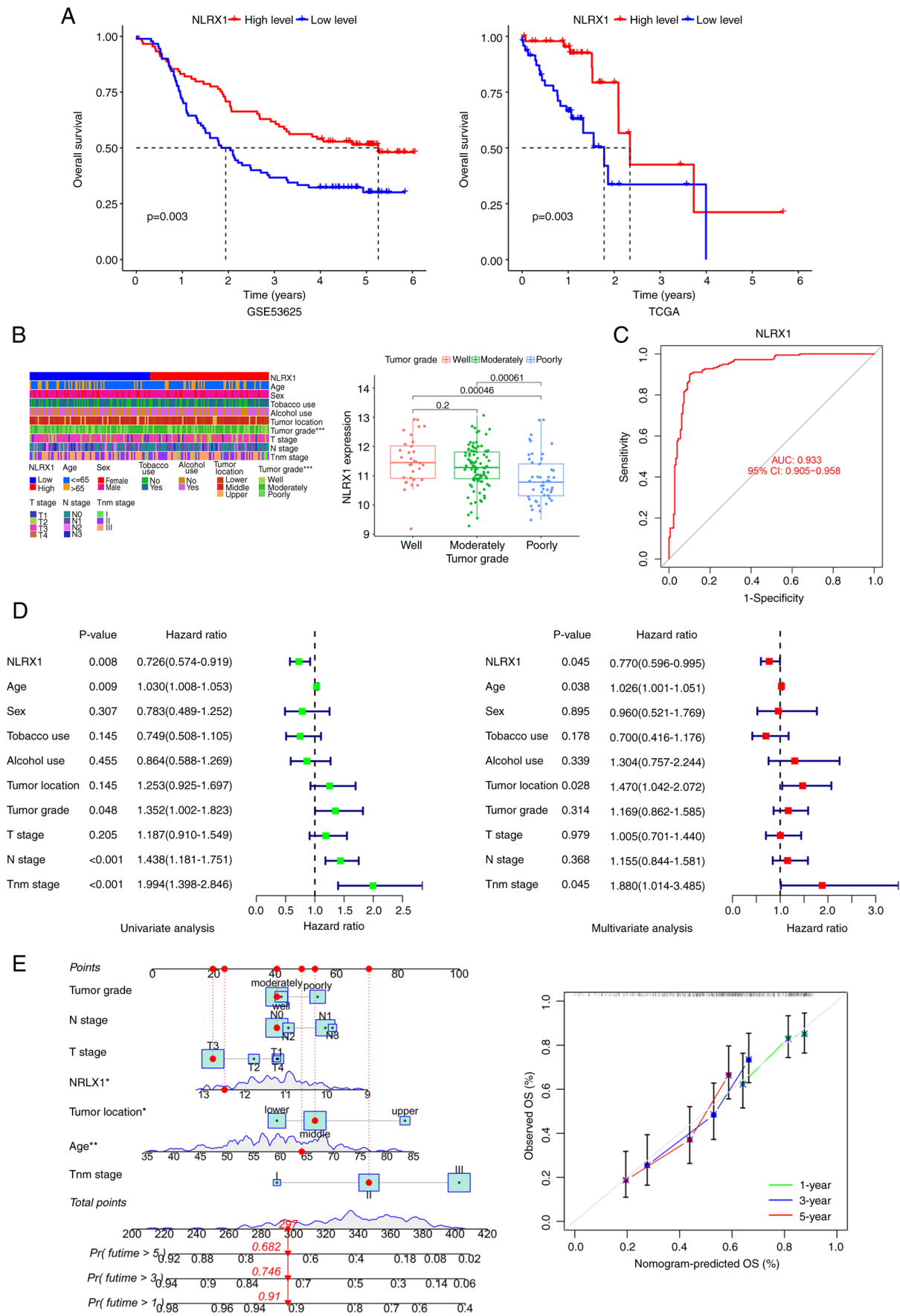


Figure 2. Clinical and prognostic value of NLRX1 in esophageal squamous cell carcinoma. (A) OS analysis. (B) Association analysis between NLRX1 and clinical pathological parameters. (C) ROC analysis. (D) Univariate and multivariate Cox regression analysis. Hazard ratios are presented with 95% CI. (E) Nomogram for OS prediction and calibration curves of the nomogram [Pr (future) is the OS rate after the indicated years]. \* $P < 0.05$ , \*\* $P < 0.01$ , \*\*\* $P < 0.001$ . NLRX1, nucleotide binding and oligomeric domain-like receptor X1; TCGA, The Cancer Genome Atlas; AUC, area under the ROC curve; ROC, receiver operating characteristic; OS, overall survival.

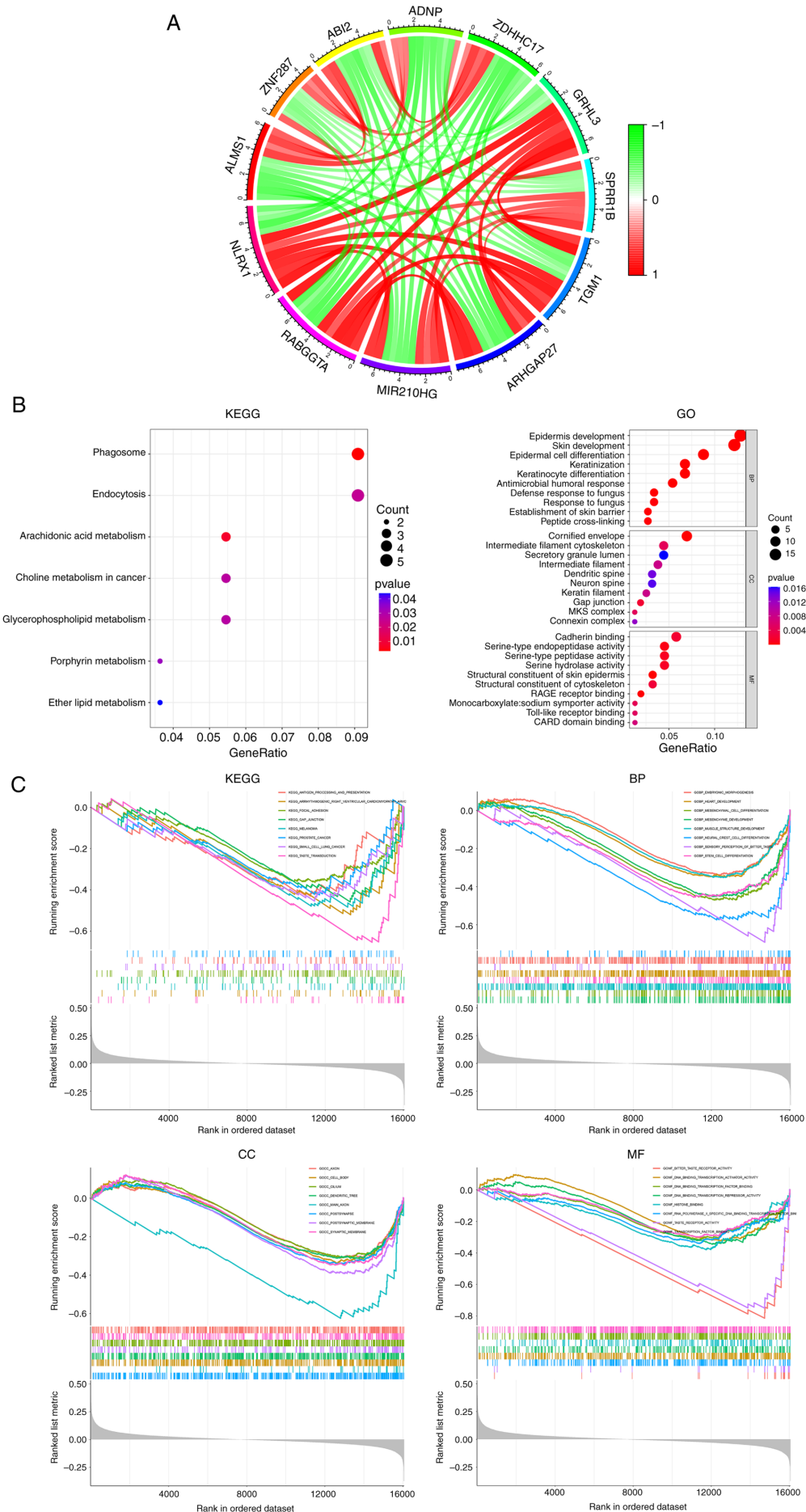


Figure 3. Continued.



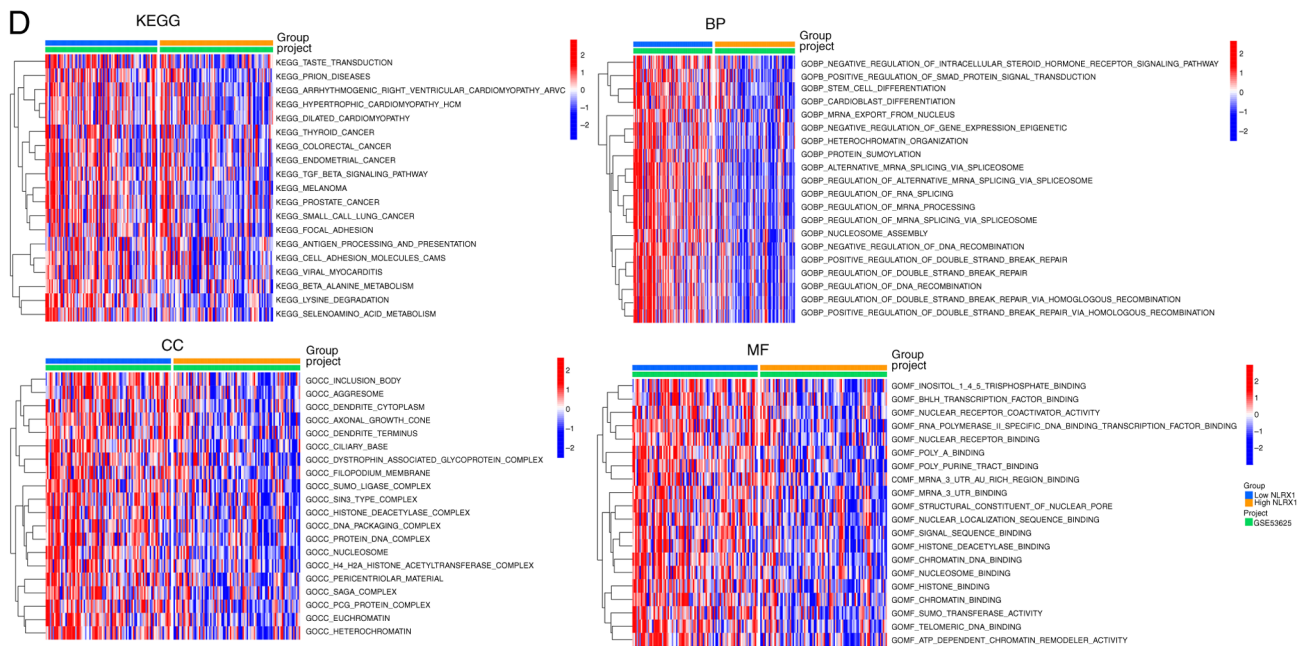


Figure 3. Identification of relevant genes for NLRX1 and enrichment analysis. (A) Circos plot showing links between NLRX1 and 11 genes in esophageal squamous cell carcinoma. (B) GO and KEGG analysis of related genes. (C) Gene-set enrichment analysis results for the low NLRX1 expression group. (D) Gene Set Variation Analysis results. NLRX1, nucleotide binding and oligomeric domain-like receptor X1; GO, Gene Ontology; KEGG, Kyoto Encyclopedia of Genes and Genomes; MF, molecular function; CC, cellular component; BP, biological process.

significantly inhibited the activation of the PI3K/AKT pathway (Fig. 7B,  $P < 0.05$ ).

## Discussion

In the present study, it was confirmed that NLRX1 functions as a tumor suppressor in ESCC using bioinformatics analysis and experiments, and its potential biological activities and regulatory mechanisms were investigated. These findings suggest that NLRX1 is crucial for the emergence and progression of ESCC.

Through data mining, it was found that NLRX1 is less expressed in ESCC at the mRNA level, and subsequently, the findings were validated at the protein level using immunohistochemistry experiments. The data from GSE53625 and TCGA both indicated that patients with low NLRX1 expression have poor prognosis. The prognostic significance of NLRX1 has also been confirmed in other cancer types. For instance, reduced expression of NLRX1 is associated with poor prognosis in cholangiocarcinoma and liver cancer (13,27,28). The clinical correlation analysis of GSE53625 with a larger data volume showed an association with tumor grading, ROC analysis demonstrated good diagnostic value, and Cox analysis also indicated that it is an independent prognostic factor for ESCC. These data indicate that NLRX1 has significant diagnostic and prognostic value in ESCC.

According to previous studies, NLRX1 is closely linked to both physiological and pathological immune, inflammatory, autophagic, mitochondrial and metabolic activities (5). To determine the function of NLRX1 in ESCC, a correlation analysis and enrichment analysis were conducted. Among the 11 genes highly correlated with NLRX1, the positively correlated GRHL3 was previously shown to inhibit tumor

growth in ESCC (29,30), further strengthening our evidence of NLRX1's tumor suppressive function in ESCC. KEGG analysis suggested that genes highly correlated with NLRX1 are mainly enriched in the phagosome, endocytosis, choline metabolism in cancer, porphyrin metabolism and lipid metabolism, which are crucial in the onset and progression of cancer (31-34). GO analysis indicated that NLRX1-related genes are associated with functions such as antifungal immunity. The phagocytosis performed by phagosomes is the core mechanism for inflammation and defense against infection factors, and there are multiple interaction points between phagosomes and endocytic pathways (35). In the present study, it was speculated that one possible pathway by which NLRX1 affects immune function is by regulating phagocytic activity, which requires further research to confirm. Previous literature has reported that NLRX1 can regulate lipid metabolism, including pomegranate acid and docosahexaenoic acid (5), which is consistent with the results of the present study. The pathway analysis results of the GSEA and GSVA showed that multiple cancer-related functional pathways, including melanoma, prostate cancer and small cell lung cancer, were enriched in the low expression group of NLRX1, indicating that NLRX1 deficiency has a certain role in the malignant development of ESCC. In recent years, there has been an increase in interest in the role of the tumor immunological microenvironment in the incidence and progression of malignancies. The innate immune response to viral infection is reportedly weakened by NLRX1 through several signaling pathways (5). However, it is unclear whether NLRX1 contributes significantly to the immune system in ESCC. Analysis of immune-related functions showed that in the low expression group of NLRX1, CCR, DCs, pDCs and T-cell co-stimulation scores were decreased, indicating that immune function

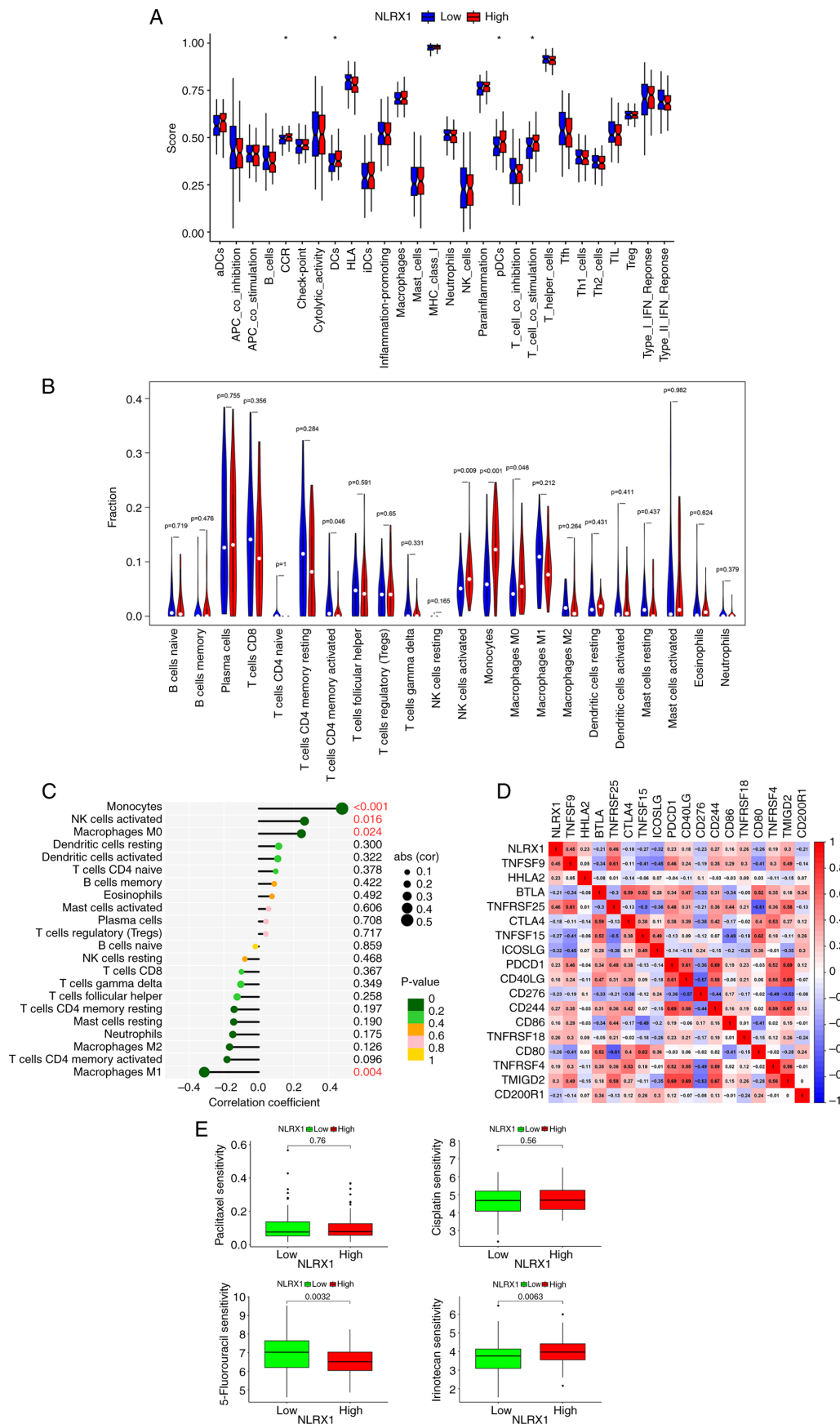


Figure 4. Immunological and drug sensitivity analysis. (A) Boxplot indicating differences in NLRX1 expression among 28 immune-related functions. (B) Violin plot showing differences in NLRX1 expression among 22 immune cell types. (C) Lollipop plot indicating the correlation between NLRX1 expression and immune-cell infiltration Definitions are provided in Table SII. (D) Correlation between NLRX1 and immune checkpoint-related genes. The numbers are the correlations coefficients and the colours indicate whether and to what extent they are negative or positive. (E) The relationship between the sensitivity of four drugs and the expression of NLRX1. \*P<0.05. NLRX1, nucleotide binding and oligomeric domain-like receptor X1; Abs (cor), absolute value of the correlation coefficient.

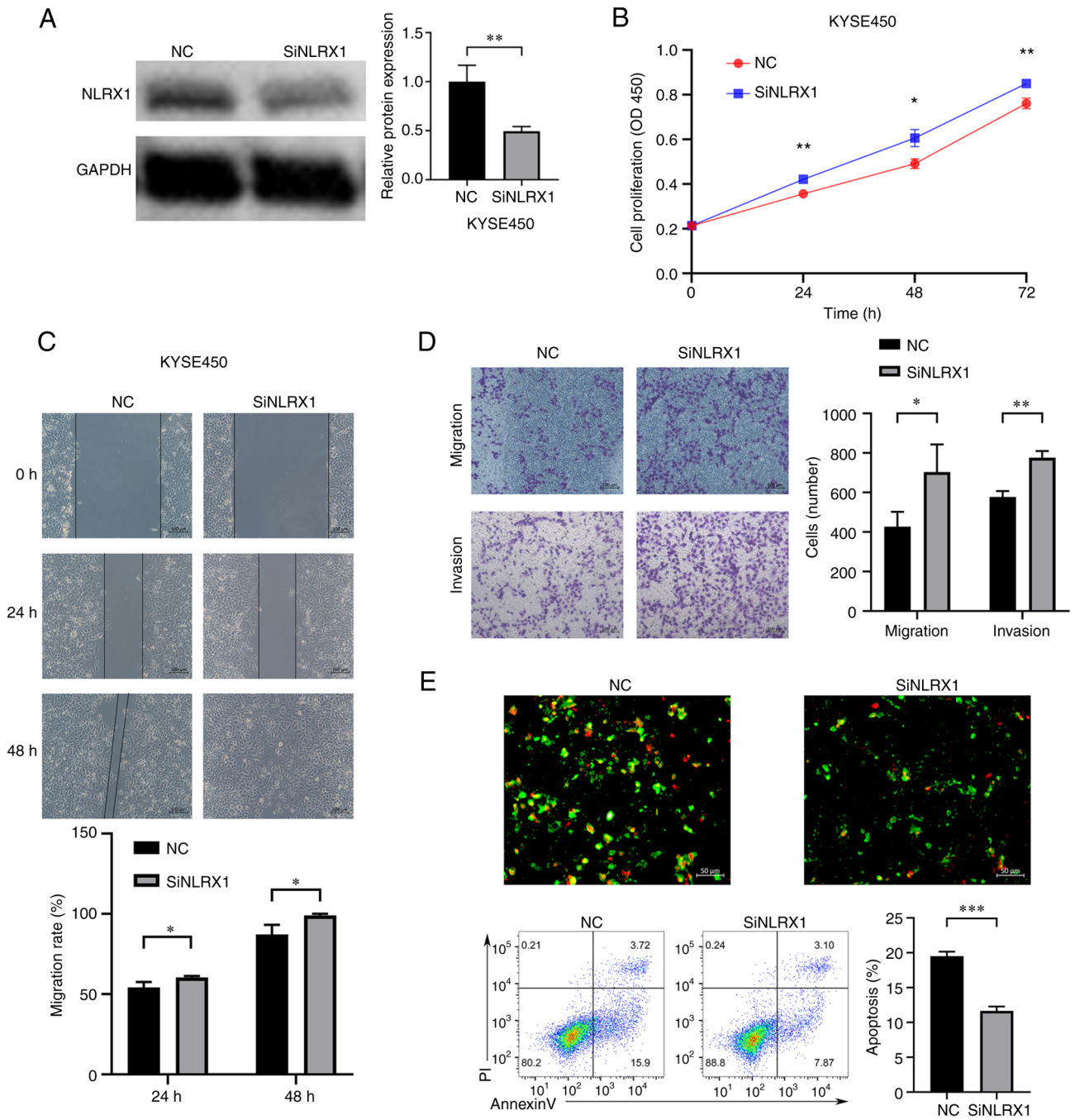


Figure 5. Downregulation of NLRX1 expression promotes the growth and development of KYSE450 cells. (A) WB results demonstrate knockdown efficiency. (B) Determination of the effect of NLRX1 on the proliferation of KYSE450 cells through Cell Counting Kit-8 assays. (C) Evaluation of the effect of NLRX1 on KYSE450 cell migration using the scratch wound-healing assay (scale bar, 100  $\mu$ m). (D) Evaluation of the impact of NLRX1 on KYSE450 cell migration and invasion by the Transwell assay (scale bar, 100  $\mu$ m). (E) Evaluation of the effect of NLRX1 on KYSE450-cell apoptosis through fluorescence microscopy (scale bar, 50  $\mu$ m; green fluorescence represents cell membrane staining and red fluorescence represents cell nuclear staining. Cells exhibiting only green fluorescence represent early apoptotic cells, while cells exhibiting only red fluorescence represented necrotic cells and cells exhibiting both red and green fluorescence represent late apoptotic cells) and flow cytometry. \* $P$ <0.05, \*\* $P$ <0.01, \*\*\* $P$ <0.001. NLRX1, nucleotide binding and oligomeric domain-like receptor X1; NC, negative control; siNLRX1, small interfering RNA targeting NLRX1; OD450, optical density at 450 nm; P-AKT, phosphorylated AKT; PI, propidium iodide; WB, western blot.

was suppressed in the low expression group of NLRX1. The differential analysis and correlation test of immune infiltration showed that NLRX1 was highly positively correlated with 'NK cells activated', 'Monocyte' and 'Macrophages M0'. 'NK cells activated' have a powerful anti-tumor effect, 'Monocyte' appears to have both pro-cancer and anti-cancer effects, and 'Macrophages M0', also known as immature macrophages,

display a phagocytic function and identify pathogenic agents (36-39). NLRX1 may affect the tumor immune micro-environment by regulating the activity of these immune cells, thereby affecting tumor occurrence and development. The present study also found a high correlation between NLRX1 and immune checkpoint receptors. For instance, TNFRSF25 and TNFSF9 are significantly positively correlated with



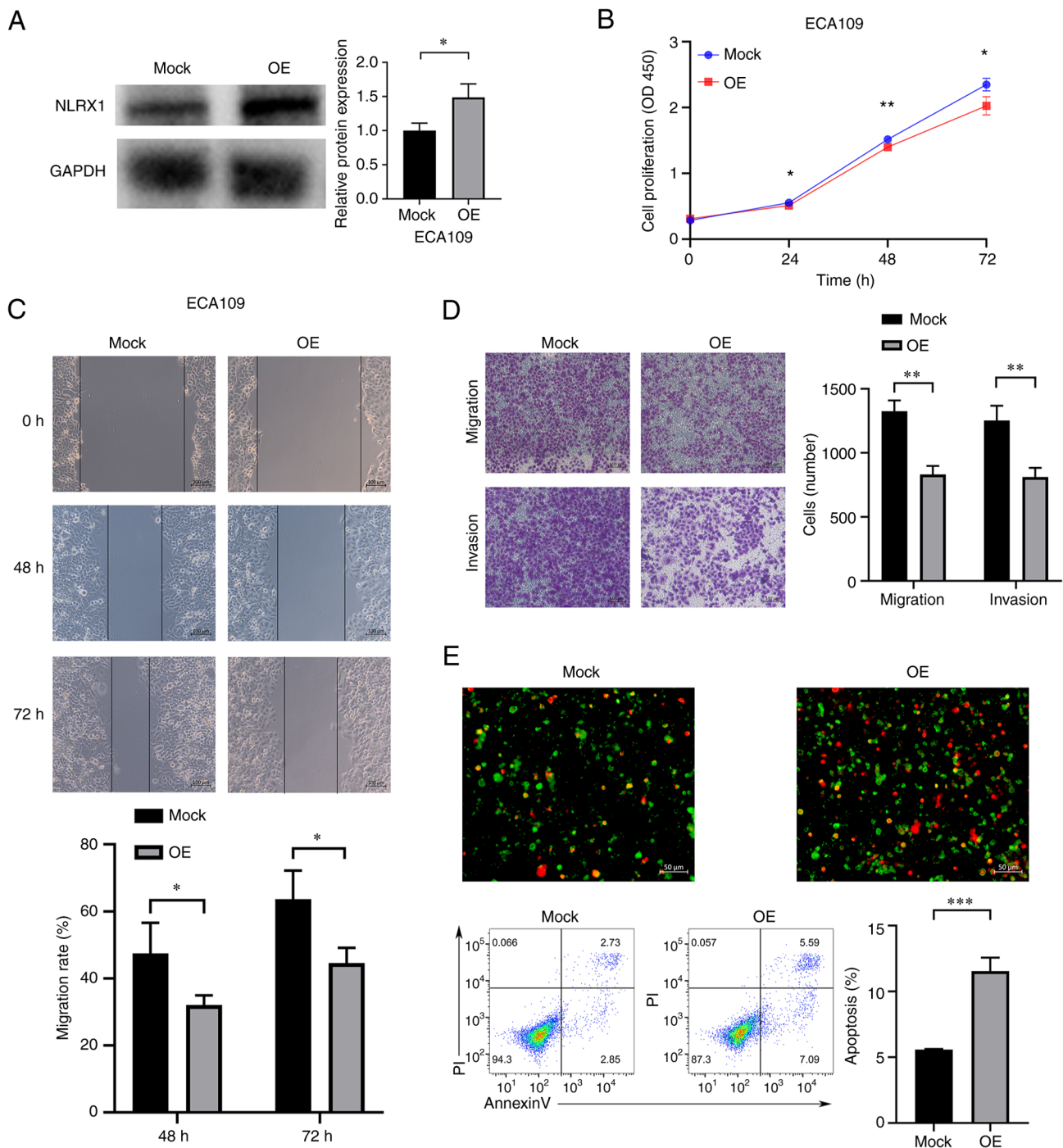


Figure 6. Upregulation of NLRX1 expression inhibits the growth and development of ECA109 cells. (A) WB results demonstrate overexpression efficiency. (B) Determination of the effect of NLRX1 on the proliferation of ECA109 cells through Cell Counting Kit-8 assays. (C) Evaluation of the effect of NLRX1 on ECA109 cell migration using the scratch wound-healing assay (scale bar, 100  $\mu$ m). (D) Evaluation of the impact of NLRX1 on ECA109 cell migration and invasion by the Transwell assay (scale bar, 100  $\mu$ m). (E) Evaluation of the effect of NLRX1 on ECA109-cell apoptosis through fluorescence microscopy (scale bar, 50  $\mu$ m; green fluorescence represents cell membrane staining and red fluorescence represents cell nuclear staining. Cells exhibiting only green fluorescence represent early apoptotic cells, while cells exhibiting only red fluorescence represented necrotic cells and cells exhibiting both red and green fluorescence represent late apoptotic cells) and flow cytometry. \* $P < 0.05$ , \*\* $P < 0.01$ , \*\*\* $P < 0.001$ . NLRX1, nucleotide binding and oligomeric domain-like receptor X1; OE, overexpression; OD450, optical density at 450 nm; PI, propidium iodide; WB, western blot.

NLRX1. TNFRSF25, also known as death receptor 3, can promote inflammation and survival through different pathways and also mediate caspase-dependent cell apoptosis. A study reported that the use of taurolidine can promote apoptosis in KYSE270 ESCC cells, which upregulates the expression of TNFRSF25 (40); therefore, it may be speculated that NLRX1 inhibiting cell proliferation and increasing apoptosis may be

related to the regulation of immune checkpoint-related genes, including TNFRSF25, which needs further confirmation. It is a co-stimulatory molecule of T cells and innate lymphoid cell (41). Considering that the low expression group of NLRX1 had lower T-cell co-stimulation scores, NLRX1 may affect its function by affecting the expression of TNFRSF25. Another example is TNFRSF9, which can mediate anti-tumor and

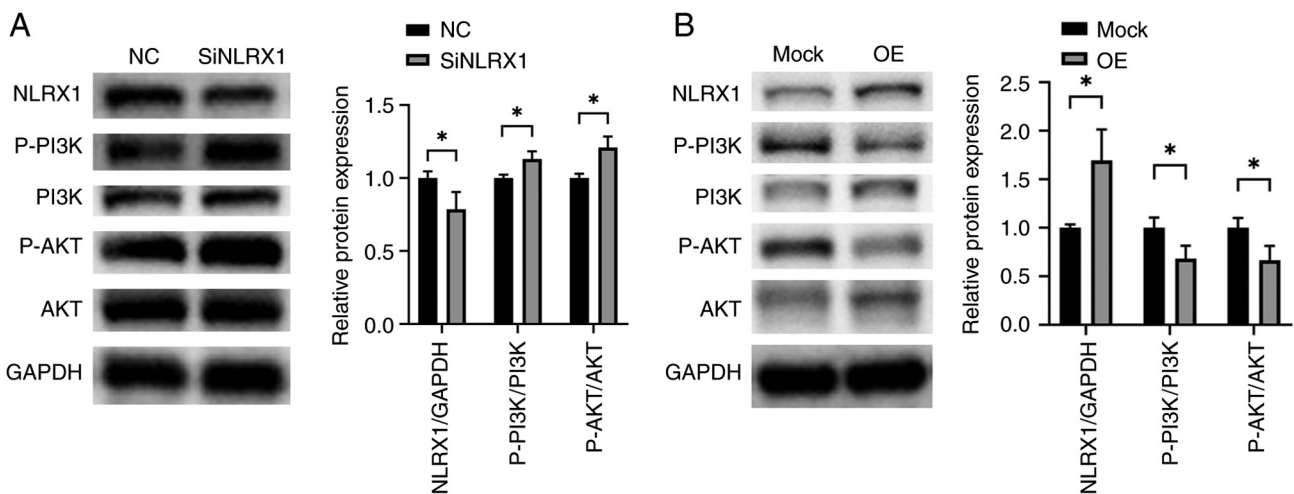


Figure 7. NLRX1 regulates the PI3K/AKT signaling pathway in esophageal squamous cell carcinoma. (A) Evaluation of the impact of NLRX1 on the PI3K/AKT pathway in KYSE450 cells measured through WB experiments. (B) Evaluation of the impact of NLRX1 on the PI3K/AKT pathway in ECA109 cells measured through WB experiments. \* $P < 0.05$ . NLRX1, nucleotide binding and oligomeric domain-like receptor X1; NC, negative control; siNLRX1, small interfering RNA targeting NLRX1; OE, overexpression; P-AKT, phosphorylated AKT; WB, western blot.

tumor-promoting signals in immune cells. Its dual function has also been observed in different solid tumor cells; however, previous studies have not yet included ESCC (42). NLRX1 may also exert its antitumor effect by affecting its expression. In conclusion, the relationship between NLRX1 and immunity of tumor patients requires further study. In addition, the relationship between NLRX1 and commonly used chemotherapy drugs for ESCC treatment in clinical practice was analyzed. The low NLRX1 group was more sensitive to irinotecan, indicating that ESCC with low expression of NLRX1 may achieve better efficacy when combined with irinotecan and other drugs. Patients with ESCC with low NLRX1 expression may obtain a better curative effect by using the treatment scheme combined with irinotecan. In summary, the present results strongly demonstrate the potential of NLRX1 as an anti-tumor therapeutic target.

NLRX1 has a role in promoting or inhibiting cancer in different solid tumors. NLRX1 is expressed more strongly in triple-negative breast cancer cells and metastatic breast cancers than it is in ER/PR+ breast cancer cells. In HeLa human cervical cancer cells and MCF-7 human ER/EP- breast cancer cells, overexpression of NLRX1 increases cell death and reduces ATP production, and overexpression of NLRX1 in MCF-7 cells reduces cell proliferation and migration (6). In MDA-MB-1 human ER/EP+ breast cancer cells, knockdown of NLRX1 results in decreased cell proliferation, migration, ATP production and inhibited TNF- $\alpha$ -induced mitochondrial autophagy. It is thought that the elevated expression of NLRX1 in invasive breast cancer supports its tumorigenic potential by controlling mitochondrial metabolic activity and turnover, preserving energy balance and preserving organelle function via mitochondrial autophagy (7). The latest research has also confirmed that NLRX1 inhibits the growth and development of Pan02 mouse pancreatic cancer cells (14). The present study on the phenotypic effects of NLRX1 on KYSE450 and ECA109 cells is consistent with this. The present study found that NLRX1 negatively regulates the growth and development of ESCC cells, which is

consistent with the function found in pancreatic cancer, liver cancer and histiocytic sarcoma (11,13,14). The expression and functional differences of NLRX1 in different cells may depend on multiple complex factors. Although NLRX1 has different roles in different tumors, its biological pathway of aggregation is consistent across different models (14). Specifically, its pathways of action in various tumors seem to be mainly attributed to NF- $\kappa$ B and AKT signal transduction (10-12,43,44). There are also literature reports indicating that it is related to MAPK, STAT3 and IL-6 signaling (12,14). Through WB assays, it was indicated in the present study that PI3K/AKT signaling is crucial to NLRX1's function in ESCC.

The present study has certain limitations. First, the bioinformatics analysis data have not been experimentally validated and using only one siNLRX1 subclone in all phenotype experiments is a limitation. The impact of NLRX1 on cell proliferation was only confirmed using the CCK-8 assay but not by other experiments specifically designed to detect cell proliferation. Furthermore, the deeper mechanisms by which NLRX1 regulates the occurrence and development of ESCC remain to be explored. Finally, the clinicopathological information of the cohort used in this study was not recorded or missing, so the clinicopathological information of this cohort could not be obtained for analysis, and a larger patient cohort is needed to validate the clinical value of NLRX1.

In conclusion, the present study found that NLRX1 is a tumor suppressor factor in ESCC. Low NLRX1 expression is a poor prognostic factor for patients with ESCC. NLRX1 affects the occurrence and development of ESCC through various pathways, including immunity and the PI3K/AKT pathway. Research on NLRX1 may provide new insights for the treatment of ESCC.

#### Acknowledgements

Not applicable.

## Funding

No funding was received.

## Availability of data and materials

The data generated in the present study may be requested from the corresponding author.

## Authors' contributions

LZ and ZL conceived and designed the study. LG, CS and AC performed the literature search, and performed the experiments and data extraction. MY analyzed and interpreted the data. LZ drafted the manuscript. LZ and ZL confirm the authenticity of all the raw data and revised the final version of the manuscript. All authors have read and approved the final manuscript.

## Ethics approval and consent to participate

The study was conducted in accordance with the Declaration of Helsinki and approved by the Second Affiliated Hospital of Zhengzhou University Ethical Review Committee (Zhengzhou, China; approval no. 2023056). All patient specimens used were obtained with the patients' informed consent.

## Patient consent for publication

Not applicable.

## Competing interests

The authors declare that they have no competing interests.

## References

- Sung H, Ferlay J, Siegel RL, Laversanne M, Soerjomataram I, Jemal A and Bray F: Global cancer statistics 2020: GLOBOCAN estimates of incidence and mortality worldwide for 36 cancers in 185 countries. *CA Cancer J Clin* 71: 209-249, 2021.
- Morgan E, Soerjomataram I, Rungay H, Coleman HG, Thrift AP, Vignat J, Laversanne M, Ferlay J and Arnold M: The global landscape of esophageal squamous cell carcinoma and esophageal adenocarcinoma incidence and mortality in 2020 and projections to 2040: New estimates from GLOBOCAN 2020. *Gastroenterology* 163: 649-658.e642, 2022.
- Zhang Y, Zhang Y, Peng L and Zhang L: research progress on the predicting factors and coping strategies for postoperative recurrence of esophageal cancer. *Cells* 12: 114, 2022.
- Gharagozloo M, Gris KV, Mahvelati T, Amrani A, Lukens JR and Gris D: NLR-dependent regulation of inflammation in multiple sclerosis. *Front Immunol* 8: 2012, 2017.
- Liu M, Liu K, Cheng D, Zheng B, Li S and Mo Z: The regulatory role of NLRX1 in innate immunity and human disease. *Cytokine* 160: 156055, 2022.
- Singh K, Poteryakhina A, Zheltukhin A, Bhatelia K, Prajapati P, Sripada L, Tomar D, Singh R, Singh AK, Chumakov PM and Singh R: NLRX1 acts as tumor suppressor by regulating TNF- $\alpha$  induced apoptosis and metabolism in cancer cells. *Biochim Biophys Acta* 1853: 1073-1086, 2015.
- Singh K, Roy M, Prajapati P, Lipatova A, Sripada L, Gohel D, Singh A, Mane M, Godbole MM, Chumakov PM and Singh R: NLRX1 regulates TNF- $\alpha$ -induced mitochondria-lysosomal crosstalk to maintain the invasive and metastatic potential of breast cancer cells. *Biochim Biophys Acta Mol Basis Dis* 1865: 1460-1476, 2019.
- Luo X, Donnelly CR, Gong W, Heath BR, Hao Y, Donnelly LA, Moghbeli T, Tan YS, Lin X, Bellile E, *et al*: HPV16 drives cancer immune escape via NLRX1-mediated degradation of STING. *J Clin Invest* 130: 1635-1652, 2020.
- Soares F, Tattoli I, Rahman MA, Robertson SJ, Belcheva A, Liu D, Streutker C, Winer S, Winer DA, Martin A, *et al*: The mitochondrial protein NLRX1 controls the balance between extrinsic and intrinsic apoptosis. *J Biol Chem* 289: 19317-19330, 2014.
- Tattoli I, Killackey SA, Foerster EG, Molinaro R, Maisonneuve C, Rahman MA, Winer S, Winer DA, Streutker CJ, Philpott DJ and Girardin SE: NLRX1 acts as an epithelial-intrinsic tumor suppressor through the modulation of TNF-mediated proliferation. *Cell Rep* 14: 2576-2586, 2016.
- Coutermarsh-Ott S, Simmons A, Capria V, LeRoith T, Wilson JE, Heid B, Philipson CW, Qin Q, Hontecillas-Magarzo R, Bassaganya-Riera J, *et al*: NLRX1 suppresses tumorigenesis and attenuates histiocytic sarcoma through the negative regulation of NF- $\kappa$ B signaling. *Oncotarget* 7: 33096-33110, 2016.
- Koblansky AA, Truax AD, Liu R, Montgomery SA, Ding S, Wilson JE, Brickey WJ, Mühlbauer M, McFadden RM, Hu P, *et al*: The innate immune receptor NLRX1 functions as a tumor suppressor by reducing colon tumorigenesis and key tumor-promoting signals. *Cell Rep* 14: 2562-2575, 2016.
- Hu B, Ding GY, Fu PY, Zhu XD, Ji Y, Shi GM, Shen YH, Cai JB, Yang Z, Zhou J, *et al*: NOD-like receptor X1 functions as a tumor suppressor by inhibiting epithelial-mesenchymal transition and inducing aging in hepatocellular carcinoma cells. *J Hematol Oncol* 11: 28, 2018.
- Nagai-Singer MA, Morrison HA, Woolls MK, Leedy K, Imran KM, Tupik JD and Allen IC: NLRX1 functions as a tumor suppressor in Pan02 pancreatic cancer cells. *Front Oncol* 13: 1155831, 2023.
- Hu N, Clifford RJ, Yang HH, Wang C, Goldstein AM, Ding T, Taylor PR and Lee MP: Genome wide analysis of DNA copy number neutral loss of heterozygosity (CNNLOH) and its relation to gene expression in esophageal squamous cell carcinoma. *BMC Genomics* 11: 576, 2010.
- Hyland PL, Zhang H, Yang Q, Yang HH, Hu N, Lin SW, Su H, Wang L, Wang C, Ding T, *et al*: Pathway, in silico and tissue-specific expression quantitative analyses of oesophageal squamous cell carcinoma genome-wide association studies data. *Int J Epidemiol* 45: 206-220, 2016.
- Liu J, Wang Y, Chu Y, Xu R, Zhang D and Wang X: Identification of a TLR-induced four-lncRNA signature as a novel prognostic biomarker in esophageal carcinoma. *Front Cell Dev Biol* 8: 649, 2020.
- Hu N, Wang C, Zhang T, Su H, Liu H, Yang HH, Giffen C, Hu Y, Taylor PR and Goldstein AM: CSMD1 shows complex patterns of somatic copy number alterations and expressions of mRNAs and target Micro RNAs in esophageal squamous cell carcinoma. *Cancers (Basel)* 14: 5001, 2022.
- Team RCM: R: A language and environment for statistical computing. 12014.
- Sepulveda JL: Using R and bioconductor in clinical genomics and transcriptomics. *J Mol Diagn* 22: 3-20, 2020.
- Ritchie ME, Phipson B, Wu D, Hu Y, Law CW, Shi W and Smyth GK: limma powers differential expression analyses for RNA-sequencing and microarray studies. *Nucleic Acids Res* 43: e47, 2015.
- Subramanian A, Tamayo P, Mootha VK, Mukherjee S, Ebert BL, Gillette MA, Paulovich A, Pomeroy SL, Golub TR, Lander ES and Mesirov JP: Gene set enrichment analysis: A knowledge-based approach for interpreting genome-wide expression profiles. *Proc Natl Acad Sci USA* 102: 15545-15550, 2005.
- Hänzelmann S, Castelo R and Guinney J: GSEA: Gene set variation analysis for microarray and RNA-seq data. *BMC Bioinformatics* 14: 7, 2013.
- Zhou L, Gan L and Liu Z: Expression and prognostic value of AIM1L in esophageal squamous cell carcinoma. *Medicine (Baltimore)* 102: e34677, 2023.
- An J, Chen X, Chen W, Liang R, Reinach PS, Yan D and Tu L: MicroRNA expression profile and the role of miR-204 in corneal wound healing. *Invest Ophthalmol Vis Sci* 56: 3673-3683, 2015.
- Zou Y, Wu F, Liu Q, Deng X, Hai R, He X and Zhou X: Downregulation of miRNA-328 promotes the angiogenesis of HUVECs by regulating the PIM1 and AKT/mTOR signaling pathway under high glucose and low serum condition. *Mol Med Rep* 22: 895-905, 2020.



27. Zhang ZJ, Huang YP, Liu ZT, Wang YX, Zhou H, Hou KX, Tang JW, Xiong L, Wen Y and Huang SF: Identification of immune related gene signature for predicting prognosis of cholangiocarcinoma patients. *Front Immunol* 14: 1028404, 2023.
28. Wang X, Yang C, Liao X, Han C, Yu T, Huang K, Yu L, Qin W, Zhu G, Su H, *et al*: NLRX and NLRX gene family mRNA expression and prognostic value in hepatocellular carcinoma. *Cancer Med* 6: 2660-2672, 2017.
29. Liang G, Wang H, Shi H, Zhu M, An J, Qi Y, Du J, Li Y and Gao S: Porphyromonas gingivalis promotes the proliferation and migration of esophageal squamous cell carcinoma through the miR-194/GRHL3/PTEN/Akt axis. *ACS Infect Dis* 6: 871-881, 2020.
30. Georgy SR, Rudiatmoko DR, Auden A, Partridge D, Butt T, Srivastava S, Wong N, Swaroop D, Carpinelli MR, Yan F, *et al*: Identification of a novel GRHL3/HOPX/Wnt/ $\beta$ -catenin proto-oncogenic axis in squamous cell carcinoma of the esophagus. *Cell Mol Gastroenterol Hepatol* 15: 1051-1069, 2023.
31. Mellman I and Yarden Y: Endocytosis and cancer. *Cold Spring Harb Perspect Biol* 5: a016949, 2013.
32. Sonkar K, Ayyappan V, Tressler CM, Adelaja O, Cai R, Cheng M and Glunde K: Focus on the glycerophosphocholine pathway in choline phospholipid metabolism of cancer. *NMR Biomed* 32: e4112, 2019.
33. Fiorito V, Chiabrando D, Petrillo S, Bertino F and Tolosano E: The multifaceted role of heme in cancer. *Front Oncol* 9: 1540, 2019.
34. Bian X, Liu R, Meng Y, Xing D, Xu D and Lu Z: Lipid metabolism and cancer. *J Exp Med* 218: e20201606, 2021.
35. Tjelle TE, Lovdal T and Berg T: Phagosome dynamics and function. *Bioessays* 22: 255-263, 2000.
36. Wu SY, Fu T, Jiang YZ and Shao ZM: Natural killer cells in cancer biology and therapy. *Mol Cancer* 19: 120, 2020.
37. Olingy CE, Dinh HQ and Hedrick CC: Monocyte heterogeneity and functions in cancer. *J Leukoc Biol* 106: 309-322, 2019.
38. Ugel S, Canè S, De Sanctis F and Bronte V: Monocytes in the tumor microenvironment. *Annu Rev Pathol* 16: 93-122, 2021.
39. Chaintreuil P, Kerrenneur E, Bourgoin M, Savy C, Favreau C, Robert G, Jacquel A and Auberger P: The generation, activation, and polarization of monocyte-derived macrophages in human malignancies. *Front Immunol* 14: 1178337, 2023.
40. Daigeler A, Chromik AM, Geisler A, Bulut D, Hilgert C, Krieg A, Klein-Hitpass L, Lehnhardt M, Uhl W and Mittelkötter U: Synergistic apoptotic effects of taurolidine and TRAIL on squamous carcinoma cells of the esophagus. *Int J Oncol* 32: 1205-1220, 2008.
41. Bittner S and Ehrenschröder M: Multifaceted death receptor 3 signaling-promoting survival and triggering death. *FEBS Lett* 591: 2543-2555, 2017.
42. Wu J and Wang Y: Role of TNFSF9 bidirectional signal transduction in antitumor immunotherapy. *Eur J Pharmacol* 928: 175097, 2022.
43. Fan Z, Pan J, Wang H and Zhang Y: NOD-like receptor X1, tumor necrosis factor receptor-associated factor 6 and NF- $\kappa$ B are associated with clinicopathological characteristics in gastric cancer. *Exp Ther Med* 21: 208, 2021.
44. Castaño-Rodríguez N, Kaakoush NO, Goh KL, Fock KM and Mitchell HM: The NOD-like receptor signalling pathway in Helicobacter pylori infection and related gastric cancer: A case-control study and gene expression analyses. *PLoS One* 9: e98899, 2014.



Copyright © 2024 Zhou et al. This work is licensed under a Creative Commons Attribution-NonCommercial-NoDerivatives 4.0 International (CC BY-NC-ND 4.0) License.